Neoclassical Toroidal Viscosity Calculations in Tokamaks Using a δf Monte Carlo Simulation and Their Verifications

S. Satake,[1] J.-K. Park,[2] H. Sugama,[1] and R. Kanno[1]
[1]*National Institute for Fusion Science, Toki, Gifu 509-5292, Japan*
[2]*Princeton Plasma Physics Laboratory, Princeton, New Jersey 08543, USA*
(Received 18 March 2011; published 25 July 2011)

Neoclassical toroidal viscosities (NTVs) in tokamaks are investigated using a δf Monte Carlo simulation, and are successfully verified with a combined analytic theory over a wide range of collisionality. A Monte Carlo simulation has been required in the study of NTV since the complexities in guiding-center orbits of particles and their collisions cannot be fully investigated by any means of analytic theories alone. Results yielded the details of the complex NTV dependency on particle precessions and collisions, which were predicted roughly in a combined analytic theory. Both numerical and analytic methods can be utilized and extended based on these successful verifications.

DOI: 10.1103/PhysRevLett.107.055001 PACS numbers: 52.55.Dy, 52.25.Dg, 52.65.Pp

The control of the toroidal rotation is an important issue in tokamaks and the International Thermonuclear Experimental Reactor (ITER), in order to improve the stability of the contained plasmas. Recent studies have shown that the nonaxisymmetry as small as $\delta B/B_0 \sim 10^{-4}$ can induce significant damping in toroidal rotation which otherwise would be much better maintained. Such a small level of nonaxisymmetry is inevitable in tokamaks due to imperfect magnets and therefore can change the plasma rotation and stability unexpectedly[1,2]. There is also a counterexample, as the small nonaxisymmetry can be applied for the purpose of stabilizing or destabilizing edge localized modes [3]. In either case, it is critical to predict the effects of nonaxisymmetry in tokamaks on the toroidal rotation.

The significant change of the toroidal rotation can occur when the axisymmetry is broken. When magnetic field strength cannot be expressed as $B = B(\psi, l)$ with ψ a flux surface label and l the distance along a field line, the action $J = \oint M v_{\|} dl$ of a particle cannot be conserved on the surfaces and radial drifts across the surfaces are generally expected [4]. The radial particle transport depends on species, and resulting radial currents produce $\vec{j} \times \vec{B}$ toroidal torque. The radial transport is not intrinsically ambipolar and is called nonambipolar transport in general, and the toroidal torque in tokamaks is particularly called neoclassical toroidal viscosity (NTV) torque.

The NTV torque has been observed and studied in many tokamaks [5–7], since the change of rotations is apparent when a small nonaxisymmetric perturbation is applied. However, theoretical predictions are nontrivial due to different particle orbits, precessions, and collisions. A number of theories have been developed in each limited regime to simplify or ignore other processes; the effects by passing and trapped particles are studied separately, and effects by trapped particles are studied in many different regimes, $1/\nu$ regime, $\nu_-\sqrt{\nu}$ regime, superbanana-plateau regime, and superbanana regime, assuming the pitch-angle collisions [8]. The overlapping between the regimes is significant in practice, so a combined NTV formula was also developed by Park *et al.* [9] using the Krook collisions including all precessions and bounce orbits, or a connection between NTV formulas was studied between $1/\nu$ regime and $\nu_-\sqrt{\nu}$ regime. None of these studies can cover the complexities in finite orbit widths and in Fokker-Planck collisions, which can be resolved only by a full numerical simulation. This Letter reports the first successful verifications for NTV using the FORTEC-3D [10], a δf Monte Carlo code solving the perturbed drift-kinetic equation in the presence of nonaxisymmetry in tokamaks, with the combined NTV formula by Park.

FORTEC-3D directly solves the following drift-kinetic equation for the deviation of distribution function from local Maxwellian, $\delta f = f - f_M$:

$$\left[\frac{\partial}{\partial t} + (\boldsymbol{v}_{\|} + \boldsymbol{v}_d)\cdot\boldsymbol{\nabla} + \dot{\mathcal{K}}\frac{\partial}{\partial \mathcal{K}}\right]\delta f - C_T(\delta f) = -\left(\boldsymbol{v}_d\cdot\boldsymbol{\nabla} + \dot{\mathcal{K}}\frac{\partial}{\partial \mathcal{K}}\right) f_M + C_P f_M, \quad (1)$$

where the independent phase-space variables are chosen as $(\psi, \theta, \zeta, \mathcal{K}, \mu)$, (ψ, θ, ζ) are the guiding-center position in Boozer coordinates, and $(\mathcal{K}, \mu)$ are the kinetic energy and magnetic moment, respectively. The linearized Fokker-Plank collision term is separated into the test-particle part C_T and the field-particle part C_P, which ensures the conservation laws. The guiding-center drift velocity $\boldsymbol{v}_d$ contains all the $\boldsymbol{\nabla}B$-, curvature-, and $\boldsymbol{E}\times\boldsymbol{B}$-drift terms and each simulation marker follows the exact drift orbit, including finite radial excursion, in a perturbed field.

The evaluation of the neoclassical toroidal viscosity $\langle \boldsymbol{e}_\zeta \cdot \boldsymbol{\nabla}\cdot\mathbf{P}\rangle$, where $\langle\cdots\rangle$ denotes a flux-surface averaging, $\boldsymbol{e}_\zeta = \partial\boldsymbol{x}/\partial\zeta$ is the toroidal covariant basis and $\mathbf{P}$ is the

pressure tensor,, respectively, is based on the idea by Lewandowski *et al.* [11] which utilizes the magnetic field spectrum expression. Here we use an expression in Fourier spectrum form;

$$B(\psi,\theta,\zeta) = B_0\Big[1 - \sum_{m\geq 0}\epsilon_m(\psi)\cos(m\theta) + \sum_{m\geq 0, n\neq 0}\delta_{m,n}(\psi)\cos(m\theta - n\zeta)\Big]. \quad (2)$$

By noting that the Jacobian in Boozer coordinates is proportional to B^{-2}, the flux-surface averaged toroidal viscosity can be expressed as $\langle \boldsymbol{e}_\zeta \cdot \boldsymbol{\nabla}\cdot\mathbf{P}\rangle = \langle \delta P(\partial B/\partial\zeta)/B\rangle$, where $\delta P = \int d^3v \delta f M(v_\perp^2/2 + v_\parallel^2)$. Making use of Eq. (2), we have the following form:

$$\langle \boldsymbol{e}_\zeta \cdot \boldsymbol{\nabla}\cdot\mathbf{P}\rangle = B_0 \sum_{m,n\neq 0} n\delta_{m,n}\left\langle \frac{\delta P}{B}\sin(m\theta - n\zeta)\right\rangle. \quad (3)$$

Thus NTV is evaluated directly from the perturbed distribution function δf. There is no approximation used, such as large-aspect-ratio or small-orbit-width limit expansions, which are often adopted in analytic formulae.

The primal benchmarks for zero $\boldsymbol{E}\times\boldsymbol{B}$ limit cases have been carried out recently and it was reported that the numerical scheme has good convergence even for a very weak perturbation amplitude ($\delta_{m,n}\sim 10^{-4}$) and that the $|\delta_{m,n}|^2$ dependence of NTV is confirmed [12]. It was also found that there is a discrepancy between the FORTEC-3D result with Shaing's formulae [8] as collision frequency goes lower from the so-called $1/\nu$ regime to the superbanana-plateau regime. It is expected that the difference comes from the fact that the analytic formulae are constructed by assuming a certain limited range in collisionality and thus fail to reproduce the dependence of NTV on collision frequency. Therefore, to verify the simulation results, here we conduct a benchmark of FORTEC-3D with another analytic formula [9], which gives a connection formula among different collisionality regimes.

The combined analytic formula is derived from a bounce-averaged drift-kinetic equation for the "lth class" perturbed distribution function $f_1 = f_{1l}(\mathcal{K},\mu,\psi,\alpha = q\theta - \zeta)\exp[-2i\pi lh]$,

$$i(l\omega_b - n\langle v_d^\alpha\rangle_b)f_{1l} + \langle C_l[f_{1l}]\rangle_b = \langle v_d^\psi \mathcal{P}^l\rangle_b \frac{\partial f_M}{\partial\psi}, \quad (4)$$

where $h(\mathcal{K},\mu,\theta) = (\int_0^\theta d\vartheta v_d^\alpha \mathcal{J}B/v_\parallel)/(\oint_0^\theta d\vartheta v_d^\alpha \mathcal{J}B/v_\parallel)$, $\mathcal{P}^l \equiv e^{2i\pi lh}$, $\langle A\rangle_b \equiv (\omega_b/2\pi)\oint qd\vartheta(A\mathcal{J}B/v_\parallel)$ is the bounce average of a function A with the bounce frequency $\omega_b \equiv 2\pi/\oint qd\vartheta(\mathcal{J}B/v_\parallel)$, and v_d^α and v_d^ψ are drift velocity in the α and ψ direction, respectively. The Jacobian $\mathcal{J}$ is a constant factor if Hamada coordinates are used and therefore is omitted hereafter. The precession velocity $\langle v_d^\alpha\rangle_b$ is given as follows:

$$\langle v_d^\alpha\rangle_b = -q\frac{d\Phi}{d\psi} + \frac{q}{e}\left\langle \mu\frac{\partial B}{\partial\psi} - (2\mathcal{K} - 2\mu B)\frac{d\ln B}{d\psi}\right\rangle_b, \quad (5)$$

where $\Phi(\psi)$ is the electrostatic potential which makes the $\boldsymbol{E}\times\boldsymbol{B}$ rotation. Similarly, $\langle v_d^\psi \mathcal{P}^l\rangle_b$ is given from the action $J_l \equiv \oint qd\vartheta v_\parallel B\mathcal{P}^l$ as $\langle v_d^\psi \mathcal{P}^l\rangle_b \propto \partial J_l/\partial\alpha$, where

$$\frac{\partial J_l}{\partial\alpha} = \frac{2\pi}{\omega_b}\left\langle\left(\frac{2\mathcal{K} - 3\mu B}{B}\right)\frac{\partial}{\partial\alpha}(B\mathcal{P}^l)\right\rangle_b. \quad (6)$$

Approximating the collision term by the Krook operator $C[f_1] = -\nu_K f_1$, Eq. (4) can be solved for f_{1l}, and the radial flux of the lth class particles $\Gamma_l = \langle\langle \int d\boldsymbol{v} f_{1l}\boldsymbol{v}_d\cdot\boldsymbol{\nabla}\psi\rangle\rangle$ is obtained as follows;

$$\Gamma_l^{na} = \frac{q}{4\pi^2 e^2}\int d\mathcal{K}\int d\mu\oint d\zeta\frac{\partial f_M}{\partial\psi}\left|\frac{\partial J_l}{\partial\alpha}\right|^2 \times \frac{\langle|\mathcal{P}^{-l}|^2\rangle_b \nu_K\omega_b}{(l\omega_b - n\langle v_d^\alpha\rangle_b)^2 + \nu_K^2}. \quad (7)$$

This is the radial flux induced by the broken toroidal symmetry. Since the toroidal viscosity obtained in FORTEC-3D is related to this flux $\langle \boldsymbol{e}_\zeta\cdot\boldsymbol{\nabla}\cdot\mathbf{P}\rangle = e\Gamma^{na}/q$, one can compare the calculation results from these two methods. Equation (7) is still complicated to solve, and therefore further approximations are adopted concerning the expressions for ω_b, $\langle v_d^\alpha\rangle_b$, $\partial J_l/\partial\alpha$, and ν_K by assuming a large aspect ratio, circular cross section, low collisionality, etc. (see [9]). One can see that a large contribution to NTV comes from the resonant particles which satisfy the condition $l\omega_b - n\langle v_d^\alpha\rangle_b \simeq 0$ from Eq. (7). Since the resonant particles' contribution is significant near the resonant flux surfaces where $mq(\psi) - n \simeq 0$, the analytic formula uses the approximation $mq - n \simeq 0$ in some parts. In the following benchmarks in the $\boldsymbol{E}\times\boldsymbol{B}\to\boldsymbol{0}$ limit, we adopt the $l = 0$ part of Eq. (7). It represents the contribution from particles of which ω_b is large enough to regard their bouncing orbits as almost closed. The $l \geq 1$ part will be important when the precession drift $\langle v_d^\alpha\rangle_b$ is fast enough to harmonize with the bouncing motion.

Here we should note the magnetic field model used here. We are not involved in the problems such as how much the external perturbation field penetrates into the plasma and whether or not a $\delta_{m,n}$ component creates a local magnetic island at $q = m/n$ resonant surface as discussed in [13,14]. Instead, we use a simple model, in which the perturbation field spectra are superimposed on a circular tokamak model $B = B_0(1 - \epsilon_t\cos\theta)$. Another point is about the difference in the coordinate systems, that is, FORTEC-3D is based on Boozer coordinates while Hamada coordinates are used in the analytic formula. Here it is assumed that the perturbation field spectra $\delta_{m,n}$ have the same profiles seen in the two different coordinates. As we have discussed in [12], the difference can be neglected if $\epsilon_t, \nu_* \ll 1$, and if we compare NTV around the resonant surfaces which are

not so close to the plasma edge, where ϵ_t is the inverse aspect ratio, $\nu_* = qR_0/(\epsilon_t^{3/2} v_{\rm th} \tau_i)$ is the normalized collisionality, $v_{\rm th}$ is thermal velocity, and τ_i is the ion collision time, respectively.

The geometry of the model tokamak for the benchmark is $R_0 = 10$ m, $a = 2.5$ m, $B_0 = 10$ T, and the q profile is $q(\rho) = 1.2 + 9.8\rho^3$, where $\rho = \sqrt{\psi/\psi_{\rm edge}}$ is used for the index of the flux surface. Plasma density and temperature are chosen so that ν_* becomes about 0.1 at $\rho = 0.4 \sim 1.0$. Two types of perturbation field are considered: one is the $(m, n) = (7, 3)$ single-mode case $\delta B/B_0 = \delta_{7,3}(\rho) \times \cos(7\theta - 3\zeta)$, where $\delta_{7,3} = 0.02\rho^2$, and the other is the multihelicity case in which three-mode perturbation is given as $\delta B/B_0 = \sum_{m=13,14,15} \delta_{m,3}(\rho) \cos(m\theta - 3\zeta)$, where $\delta_{m,3} = 0.005\rho^4$. To benchmark the ν_* dependence of NTV, the collisionality is artificially multiplied by a numerical factor "c_m." Here we explore $0.001 \le c_m \le 50$, or roughly $10^{-4} < \nu_* < 5$. According to the criteria by Shaing [8], $10^{-2} < \nu_* < 1$ is the $1/\nu$ regime and $\nu_* < 10^{-2}$ corresponds to the superbanana-plateau (SB-P) regime. The boundary between the SB-P and superbanana regimes, which depends on $|\delta_{m,n}|^{3/2}$, is below this range, $\nu_* < 10^{-4}$.

First, to see the dependence on collision frequency, the NTV values on several flux surfaces are plotted against ν_* in Figs. 1(a) and 1(b). The $\rho = 0.493$ result in Fig. 1(a) and $\rho = 0.706$ result in Fig. 1(b) correspond to the peak value of NTV in each case, which appears at the resonant flux surface where $q(\rho)$ is equal to m/n of the given (m, n) mode. The dependence agrees well between FORTEC-3D and the combined analytic formula, especially for the peak value at the resonant surfaces, in the wide range of plasma collisionality. In Fig. 1, the peak values of asymptotic $1/\nu$ and the superbanana-plateau limit formulae from [8] are also shown. There is no clear SB-P regime found either in FORTEC-3D or in the combined analytic formula in the region $10^{-4} < \nu_* < 10^{-2}$ where it is classified as the SB-P regime, and a large discrepancy is seen from the asymptotic formula in the lower-ν_* regime.

Next, Figs. 2 and 3 show the radial profiles of the NTV $\langle \boldsymbol{e}_\zeta \cdot \boldsymbol{\nabla} \cdot \mathbf{P} \rangle$ for the single and multihelicity cases, respectively, with the c_m factor varied. We find good agreement between the FORTEC-3D simulation and the combined analytic formula around the peak of NTV, which appears at the resonant surface (for the multihelicity case, three resonant surfaces are at $\rho \simeq 0.68$, 0.71, and 0.73.) The peak value and its position are similar between them. The NTV profile from Shaing's $1/\nu$-theory is also plotted for the $\nu_* \simeq 0.1 (c_m = 1)$ case in these figures. One can see two differences: the peak amplitude of the $1/\nu$-theory is much larger than the other two calculations, and the NTV drops very quickly at the off-resonant position, while a certain magnitude of NTV remains at the off-resonant tails in the other two calculations, especially in lower-ν_* cases of FORTEC-3D.

Although the radial profiles of NTV around the resonant position are similar between FORTEC-3D and Park's

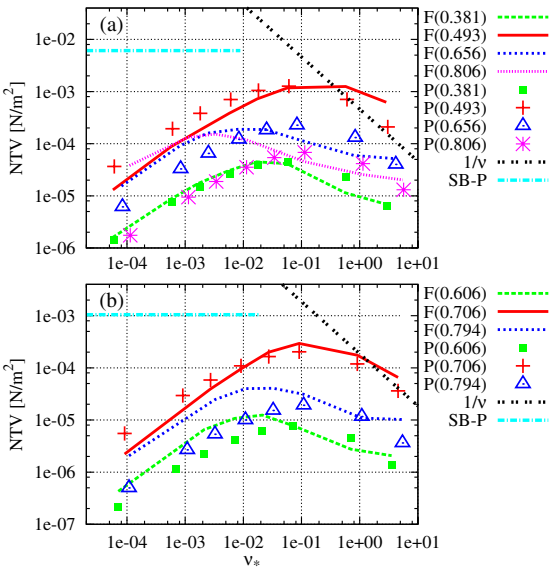

FIG. 1 (color online). Dependence of NTV on $\nu*$ at several radial positions in (a) single and (b) multihelicity cases, respectively. The "F" curves are results from FORTEC-3D, the "P" symbols are from the combined analytic formula, and the numerals denote the radial position ρ. The $1/\nu$ and SB-P lines represent the peak values from the $1/\nu$ and superbanana-plateau theory at the resonant surface, respectively.

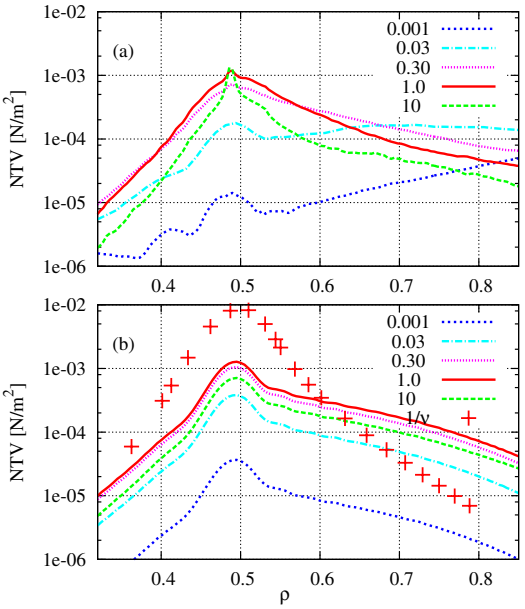

FIG. 2 (color online). Radial profiles of NTV $\langle \boldsymbol{e}_\zeta \cdot \boldsymbol{\nabla} \cdot \mathbf{P} \rangle$ calculated from (a) FORTEC-3D and (b) the combined analytic formula by Park, in the single-mode case with varying the collisionality magnification factor c_m (the numerals on the legend). For comparison, the NTV profile from the $1/\nu$-theory for the $c_m = 1.0$ case is also shown (symbols).

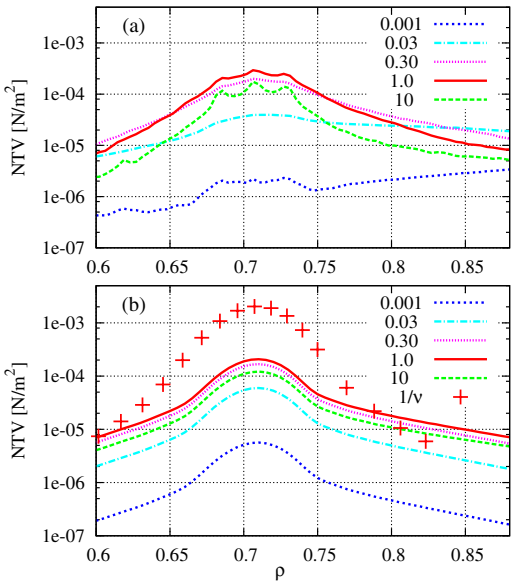

FIG. 3 (color online). Radial profiles of NTV $\langle \boldsymbol{e}_\zeta \cdot \boldsymbol{\nabla} \cdot \mathbf{P} \rangle$ calculated from (a) FORTEC-3D and (b) the analytic formula in the multihelicity case for several collisionalities.

formula, there is a difference locally for the multihelicity case. In Fig. 3, one can see three local peaks of NTV in the FORTEC-3D result, which corresponds to the three resonant surfaces, which do not appear in the results of the combined analytic formula. The local peaks are considered higher-order correction effects which are included only in the direct simulation of FORTEC-3D. We have discussed in [12] that toroidal couplings among toroidicity of the field $(m, n) = (1, 0)$, field perturbation (m, n), and the $\sin[(m \pm 1)\theta - n\zeta]$-dependent part of δP will create $O(\epsilon_t)$ corrections to NTV on each of the resonant surfaces, if the neighboring two modes (m, n) and $(m \pm 1, n)$ are applied at once. Since the height and width of the peaks in FORTEC-3D depend on the collisionality, it is also anticipated that the difference in the shape of the peak profile between the two methods results from the finite radial drift of resonant particles. The decorrelation time scale of the resonant particles is determined by the combination of collisional scattering and the collisionless detrapping process, which occurs when a resonant particle drifts radially and then escapes from the local ripples. In the analytic model, however, such a finite-orbit-width effect is not taken into account in deriving Eq. (7). This difference will be important when we discuss how the NTV torque is localized and examine its effect on the rotation profile.

Another difference between the two calculations is found at the outer off-resonant position. In Fig. 2, about a one order larger NTV is obtained in FORTEC-3D than in the analytic formula at $\rho \simeq 0.8$ when $\nu_* \ll 1$. However, we found good agreement between them at the inner off-resonant position both in single and multihelicity cases. Note here that we have neglected the difference of the coordinate systems as mentioned before. As the real difference in perturbation spectra seen in Boozer and Hamada coordinates tends to enlarge at the edge region, the difference in the NTVs at the edge might be caused by neglecting the difference in coordinates. It is important to use a proper coordinate system to express perturbation field spectra in applying these methods to realistic situations in experiments.

In conclusion, the benchmarks demonstrated that both calculation methods for NTV agree well in wide collisionality range except the edge region, and a large discrepancy is found from the asymptotic limit theories. Since in previous analyses some have reported agreement between the observation of rotation damping with the estimation of NTV from analytic theory [5] while the others have shown a difference [7], it is important to verify the NTV calculation methods before applying them to experiments. The present result encourages us to use the combined analytic formula to evaluate and analyze NTV in experiments. On the other hand, we have also found a difference between two methods in the shape of the peak profile of NTV around the resonant surface. Direct kinetic simulation of FORTEC-3D can reveal the detailed properties of NTV, which is difficult to treat analytically. Although it takes longer computation time, the direct simulation reinforces the reliability of the combined analytic formula and can be utilized to understand the physics of neoclassical viscosity in detail. We will continue to verify the calculation methods including the $\boldsymbol{E} \times \boldsymbol{B}$ rotation effect to study the physics of NTV in $\nu_- \sqrt{\nu}$ regimes, and offer them as reliable and general methods.

This work is supported in part by the Japanese Ministry of Education, Culture, Sports, Science, and Technology, Grant No. 21560861 and by the NIFS collaborative Research Programs 09KTAD006 and 10KDAT020.

[1] H. Urano *et al.*, Nucl. Fusion **47**, 706 (2007).
[2] Y. Liang *et al.*, Nucl. Fusion **50**, 025013 (2010).
[3] T. Evans *et al.*, Phys. Rev. Lett. **92**, 235003 (2004).
[4] J. R. Cary *et al.*, Phys. Plasmas **4**, 3323 (1997).
[5] W. Zhu *et al.*, Phys. Rev. Lett. **96**, 225002 (2006).
[6] M. Bécoulet *et al.*, Nucl. Fusion **49**, 085011 (2009).
[7] Y. Sun *et al.*, Plasma Phys. Controlled Fusion **52**, 105007 (2010).
[8] K. Shaing *et al.*, Nucl. Fusion **50**, 025022 (2010).
[9] J. K. Park *et al.*, , Phys. Rev. Lett. **102**, 065002 (2009).
[10] S. Satake *et al.*, Plasma Fusion Res. **3**, S1062 (2008).
[11] J. L. V. Lewandowski *et al.*, Phys. Plasmas **8**, 2849 (2001).
[12] S. Satake *et al.*, Plasma Phys. Controlled Fusion **53**, 054018 (2011).
[13] J.-k. Park *et al.*, Phys. Plasmas **16**, 056115 (2009).
[14] Y. Kikuchi *et al.*, Plasma Phys. Controlled Fusion **49**, A135 (2007).